

Approaching the Island of Inversion: ^{34}P

P. C. Bender,¹ C. R. Hoffman,¹ M. Wiedeking,^{2,3} J. M. Allmond,⁴ L. A. Bernstein,³ J. T. Burke,³ D. L. Bleuel,³ R. M. Clark,² P. Fallon,² B. L. Goldblum,⁵ T. A. Hinnners,¹ H. B. Jeppesen,² Sangjin Lee,¹ I-Y Lee,² S. R. Leshner,³ A. O. Macchiavelli,² M. A. McMahan,² D. Morris,¹ M. Perry,¹ L. Phair,² N. D. Scielzo,³ S. L. Tabor,¹ Vandana Tripathi,¹ and A. Volya¹

¹*Department of Physics, Florida State University, Tallahassee, Florida 32306*

²*Lawrence Berkeley National Laboratory, Berkeley, California 94720*

³*Lawrence Livermore National Laboratory, Livermore, CA 94551*

⁴*Department of Physics, University of Richmond, VA 23173*

⁵*Department of Nuclear Engineering,
University of California, Berkeley, CA 94720*

(Dated: June 14, 2011)

Abstract

Yrast states in ^{34}P were investigated using the $^{18}\text{O}(^{18}\text{O},\text{pn})$ reaction at energies of 20, 24, 25, 30, and 44 MeV at Florida State University and at Lawrence Berkeley National Laboratory. The level scheme was expanded, γ -ray angular distributions were measured, and lifetimes were inferred with the Doppler-shift attenuation method by detecting decay protons in coincidence with one or more γ rays. The results provide a clearer picture of the evolution of structure approaching the “Island of Inversion”, particularly how the 1 and 2 particle-hole (ph) states fall in energy with increasing neutron number approaching inversion. However, the agreement of the lowest few states with pure *sd* shell model predictions shows that the level scheme of ^{34}P is not itself inverted. Rather, the accumulated evidence indicates that the 1-ph states start at 2.3 MeV. A good candidate for the lowest 2-ph state lies at 6236 keV, just below the neutron separation energy of 6291 keV. Shell model calculations made using a small modification of the WBP interaction reproduce the negative-parity, 1-ph states rather well.

I. INTRODUCTION

A major issue in nuclear structure is how the filling of proton shells affects the neutron shell structure, and vice-versa. One of the best regions to study this effect is among nuclei in the so-called “Island of Inversion” with $Z \sim 10$ and $N \sim 20$ [1, 20]. The ground state structures of these nuclei are dominated by intruder configurations involving neutrons in orbitals above $N = 20$. That is, the level structure is inverted, with the intruder states which would normally be expected to lie higher in excitation falling below the “normal” sd states. This seems to be driven by a combination of a substantially reduced $N = 20$ shell gap for neutrons and binding energy gains for the intruder configurations due to correlation energy [3]. The tensor nucleon-nucleon force may account for the reduced $N = 20$ gap for neutron-rich nuclei, allowing the $\nu d_{3/2}$ orbital to rise with decreasing occupation of the $\pi d_{5/2}$ orbital [4]. Another way to view correlation energy in a geometrical picture is increased deformation, which allows some Nilsson orbitals arising out of the $f_{7/2}$ shell to drop below some of those from the $d_{3/2}$ orbital.

Although much progress has been made recently in understanding the island of inversion phenomenon, more questions remain which go to the heart of nuclear shell structure. Study of nuclear structure approaching the island of inversion, *i.e.* as the excited intruder states decrease towards the ground state, can shed valuable light on this problem. The empirical boundary of the island of inversion appears to be about $N - Z = 7$, where the ground states reach about 50% intruder admixture. The $Z = 15$ phosphorus isotopes provide an interesting region to study the approach to inversion because they cannot quite reach the boundary neutron excess of 7 before their neutron number exceeds 20 and $\nu f_{7/2}$ configurations become normal for the ground states. Because of its proximity to the $N = 20$ shell gap, we have investigated $N = 19$ ^{34}P in the present work. Another reason to study ^{34}P is that there has been uncertainty about the assignment of its lowest intruder state, and this state plays a crucial role in the approach to inversion, as described in Ref. [5].

Progress in unraveling the structure of ^{34}P has come slowly over the last four decades. A spin-parity assignment of 1^+ was made to the ground state from observation of its allowed β decay to known states in ^{34}S [6]. Five excited states were located in a $(t, ^3\text{He})$ measurement, but the lack of angular distributions or any reaction analysis prevented the assignment of spins [7]. At about the same time, an investigation of the β decay of ^{34}Si to states in ^{34}P

observed the same lowest two excited states and assigned 1^+ to the second excited state at 1608 keV [8]. Most of states reported in Ref. [7] were observed in a (${}^7\text{Li}, {}^7\text{Be}$) charge exchange reaction along with two higher lying levels [9]. A decade later a γ decay line was observed from the 2305 keV state in a heavy-ion reaction [10]. In agreement with an earlier speculation [7], it was suggested that this state may be a member of the intruder $\pi s_{1/2} \otimes \nu f_{7/2}$ doublet with spin parity 3^- or 4^- because heavy-ion reactions strongly favor yrast states. The advent of short-lived radioactive beams from projectile fragmentation led to a study of intermediate-energy Coulomb excitation of a ${}^{34}\text{P}$ beam using a NaI scintillator array [11]. The subsequent decay of the first excited state was observed (429 keV) along with a weaker line at 627 ± 9 keV. The latter line was interpreted as the decay of the 2225 ± 10 keV state observed in Ref. [7], but the intermediate lines at 1179 and 1607 keV were not observed, perhaps because of reduced detection efficiency for higher energy γ rays. A heavy-ion deep inelastic transfer reaction located a candidate for the second member of the intruder $\pi s_{1/2} \otimes \nu f_{7/2}$ doublet and several states above the doublet [12]. This work also suggested a candidate for the 7^+ two-quasiparticle stretched $\pi f_{7/2} \otimes \nu f_{7/2}$ configuration at 6236 keV. Figures 5-7 in Ref. [12] provide good overviews of the evolving knowledge of the phosphorus isotopes. Most of the lines reported in Ref. [12] were observed in a later experiment [13], except strangely for the 1047 keV transition which is the third strongest line in Ref. [12] and the present work. 4^+ was assigned to the 2305 keV state in Ref. [13] based on a γ linear polarization measurement. This parity assignment would negate the previous interpretation of this state as the lowest $f_{7/2}$ intruder level.

We have investigated ${}^{34}\text{P}$ using a symmetric fusion-evaporation reaction to bring in as much angular momentum as possible to populate the relatively high spin intruder states in order to learn more about the approach to inversion and resolve some conflicts in the earlier work. The opportunity arose to study this reaction at two laboratories, as described below.

II. EXPERIMENT

Excited states of ${}^{34}\text{P}$ were populated through the ${}^{18}\text{O}({}^{18}\text{O}, pn)$ reaction using a $200 \mu\text{g}/\text{cm}^2$ target of ${}^{18}\text{O}$ formed by electrolysis of water enriched to 97% in ${}^{18}\text{O}$ on an 0.0127 mm Ta backing. The target backing was chosen thick enough to stop the incident beam but thin enough to allow light charged particles to pass through with limited energy loss. Several

measurements were performed with the same target at the John D. Fox laboratory at Florida State University (FSU) and at the 88-Inch Cyclotron at Lawrence Berkeley National Laboratory (LBNL).

For the FSU experiments, the FSU Compton suppressed high-purity germanium (HPGe) array was used to detect the γ rays emitted from the reaction. The array consisted of 6 single crystal HPGe detectors and 3 four-crystal Clover detectors. Each detector was surrounded by bismuth germinate (BGO) crystals used for Compton suppression. All 3 Clover detectors, along with 2 of the single crystal Ge detectors, were placed at 90° , with 2 single crystal Ge detectors at 35° and 2 at 145° , all with respect to the beam direction and at a distance of 15 cm from the target.

In the first FSU experiment, the laboratory ^{18}O beam energy was 44 MeV. The trigger for data acquisition was two Compton-suppressed Ge signals. The second experiment used a lower beam energy of 24 MeV and the same γ detector array, along with charged particle detection. These were detected and identified in a segmented $E - \Delta E$ Si particle telescope placed after the target at 0° relative to the beam axis. Both the ΔE and E detectors were 15 mm diameter 1500 μm thick silicon wafers divided into four segments radially. The trigger required a signal from any of the four segments in the ΔE detector and a Compton-suppressed Ge signal.

A second set of experiments was carried out at LBNL using ^{18}O beams from the 88-Inch Cyclotron at energies of 20, 25, and 30 MeV on the same ^{18}O target. Charged particles from the reactions, as well as γ rays decaying from excited nuclear states, were detected by the STARS-LIBERACE detector array [14–16]. This array consists of an $E - \Delta E$ Si detector telescope and 5 HPGe Clover detectors. The Si telescope used two annular Si discs of thickness 150 μm for the ΔE detector and 1000 μm for the E detector. The detectors were separated by 3 mm and the telescope was located 3 cm downstream from the target position. The telescope had an overall detection efficiency of $\sim 20\%$ for the detection of a single proton. The 5 HPGe Clover detectors were mounted 16.5 cm from the target at angles relative to the beam direction of 40° (1), 90° (2) and 140° (2). The total γ -ray efficiency at 1 MeV was $\sim 1\%$. The data acquisition trigger for the experimental setup was a charged particle signal in both the ΔE and E detectors.

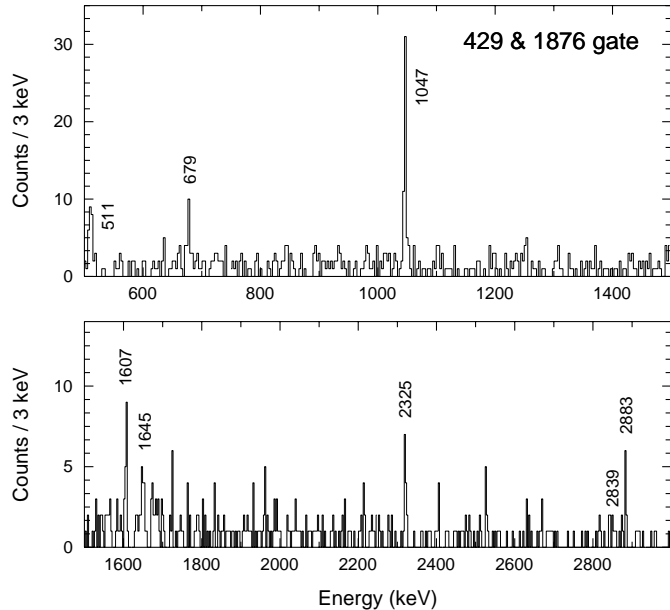


FIG. 1: The spectrum of γ rays in triple coincidence with the 429 and 1876 keV lines in ^{34}P .

III. RESULTS

An example of the data from the FSU experiments is shown in Fig. 1. It shows the γ spectrum in triple coincidence with the 429 and 1876 keV lines. The data set is a combination of both FSU experiments, but the statistics are dominated by the experiment without a proton gate. Due to the weakness of the pn exit channel, a γ triples analysis was necessary to achieve adequate spectral cleanliness in the data not gated by protons. The proton gated data, with and without a γ gate, were most valuable for studying the low-lying states.

A comparison of the relative intensities of γ lines seen at the 5 different energies is given in Table I. There is generally good agreement, keeping in mind the wide range of beam energies and the differing experimental conditions. Uncertainties in the γ energies are about 1 keV rising to about 2 keV for the lines above 2 MeV.

A. Level Scheme

The level scheme based on the $p\text{-}\gamma\text{-}\gamma$ and $\gamma\text{-}\gamma\text{-}\gamma$ coincidence relations is shown in Fig. 2. The γ -decay branches of the 1608 keV state were first observed following β decay [8]. The presence of the 1179 keV decay line from this state shows that it is populated in the present

TABLE I: Relative intensities for γ lines in ^{34}P at the indicated laboratory beam energies. The FSU data were measured at 24 and 44 MeV and the LBNL, at 20, 25, and 30 MeV. All but the 44 MeV data set were measured in coincidence with protons and normalized to the 429 keV line. The 44 MeV intensities were measured in coincidence with the 429 keV gate, so intensities of ground state decays could not be measured. Intensities in the 44 MeV data set were normalized to that of the 1876 keV line at 24 MeV.

E_x (keV)	E_γ (keV)	Relative Intensity at these energies (MeV)				
		20	24	25	30	44
429	429	100	100	100	100	
1608	1179	9(2)	5(1)	6(1)	3(1)	8(2)
	1607 ^a	6(2)	11(2)	13(2)	11(2)	
2305	1876	37(4)	76(6)	54(4)	64(4)	76(6)
2320	1891	17(2)	10(2)	15(2)	9(1)	6(1)
3352	1047	17(2)	37(4)	28(2)	44(4)	36(4)
3950	1645	11(2)	19(2)	31(2)	46(4)	20(3)
4629	679	1.0(5)	7(1)	4(1)	7(1)	9(2)
	2325	2(1)	10(2)	4(1)	10(2)	11(2)
6192	2839	< 1	6(1)	2(1)	7(1)	10(2)
6236	1607 ^a	6(2)	11(2)	13(2)	11(2)	13(2)
	2883	< 1	5(1)	3(1)	5(1)	11(2)

^aSum of the intensities of the members of the unresolved doublet except for the 44 MeV data set.

reaction, although not very strongly. We also observe the other decay branch at 1607 keV. However, except at the lowest bombarding energy, it is more, rather than less, intense than the 1179 keV line, unlike the β -decay result. More importantly, the 1607 keV line appears clearly in the 429 and 1876 keV gates (see Fig. 1), in contradiction to its sole placement as a decay to the ground state. Thus, two lines at about 1607 keV are seen in the present work. The second instance is placed near the top of the level scheme based on other coincidence relationships and intensities. The absence of any obvious differences in the centroids of the peak under different gating conditions suggests that the two members of the 1607 keV

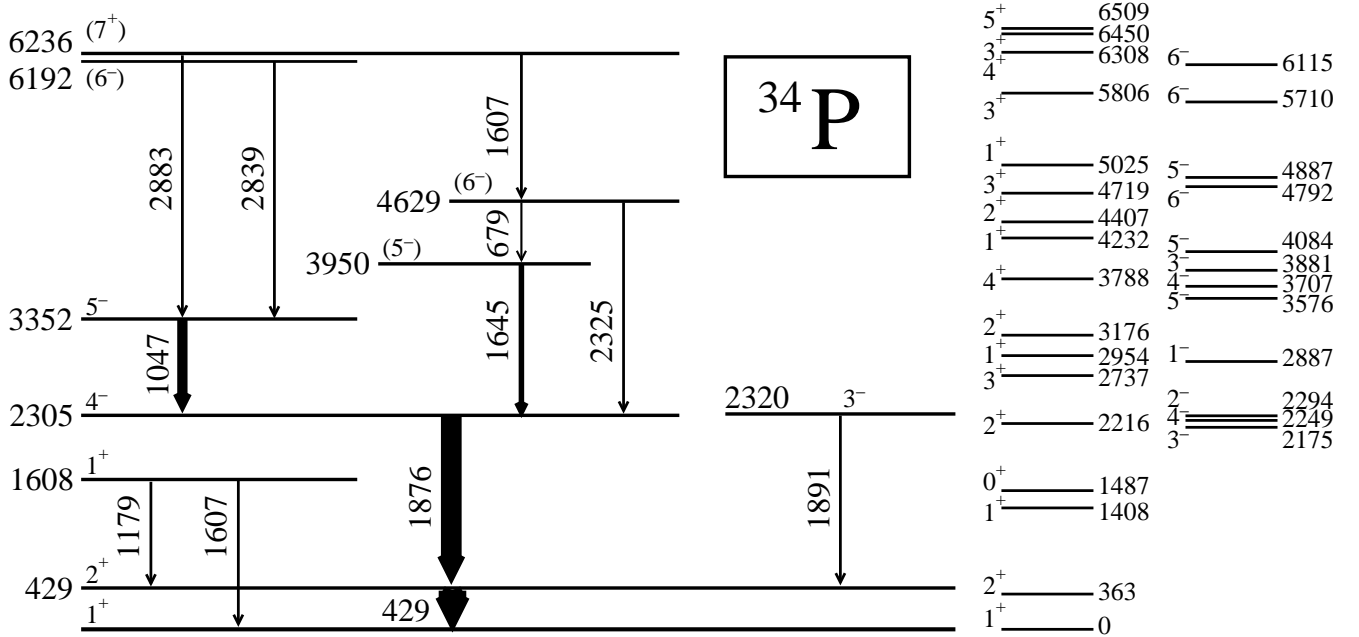


FIG. 2: The level scheme of ^{34}P based on the present data along with predictions of the shell model using the WBP-a interaction on the right.

doublet are within a keV or so of each other. Many of the levels and transitions in Fig. 2 have been reported previously, but in different and sometimes conflicting experiments, as summarized in Fig. 5 of Ref. [12]. The 679, 1645, 2325, 2839 and higher 1607 keV lines are new.

Angular distributions were fitted to the stronger lines in both the FSU and LBNL data sets. Some results are shown in Fig. 3. The spin-parity of the ground state of ^{34}P was assigned 1^+ based on its allowed β decay to known 0^+ and 2^+ states in ^{34}S [6]. It has long been suspected that the 1^+ ground state is one member of the $\pi(s_{1/2}) \otimes \nu(d_{3/2})^{-1}$ doublet and the 429 keV state is the other (2^+) member. The good fit for the $2\hbar \rightarrow 1\hbar$ spin hypothesis with relatively small mixing ratio δ for the 429 keV decay line in Fig. 3 provides confirmation of the 2^+ assignment. Spin hypotheses of 1 or 3 \hbar do not provide acceptable fits. Allowed β decay from the 0^+ ground state of ^{34}Si to the 1608 keV state provides its spin-parity assignment of 1^+ [8].

The doublet at 2305 and 2320 keV has been suggested to have an intruder configuration of $\pi s_{1/2} \otimes \nu f_{7/2}$ [12]. Our angular distribution of the 1876 keV decay line (Fig. 3) of the

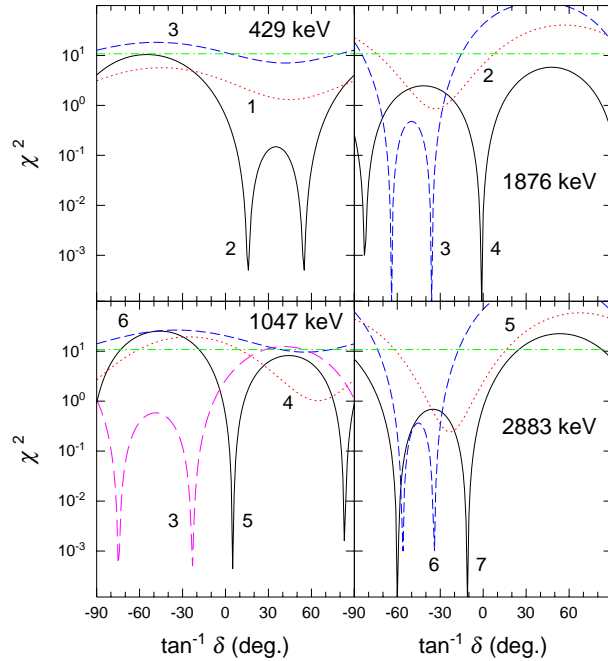


FIG. 3: (color online) Angular distribution fits for some transitions in ^{34}P . Those for the 429 and 1047 keV lines are from the LBNL data, and those for the 1876 and 2883 keV lines are from the FSU data. The spin assumptions for the upper states for each transition are indicated in the figure in units of \hbar . The spins of the lower states were fixed at 1, 4, 2, and 5 \hbar for the 429, 1047, 1876, and 2883 keV lines, respectively.

2305 keV state is consistent with an assignment of 4^- . It is also consistent with 3^+ or 4^+ , but not with 3^- because it would imply an unphysically large M2/E1 mixing ratio. The large strength to the 2305 keV state (or, more likely, the unresolved combination of the 2305 and 2320 keV states) in the $^{34}\text{S}(t,^3\text{He})$ reaction [7] also implies a neutron configuration with relatively high degeneracy like $f_{7/2}$. Our angular distribution for the 1891 keV decay of the 2320 keV state is consistent with $3^- \rightarrow 2^+$ decay, but not with $4^- \rightarrow 2^+$.

Note that the 2305 keV level was assigned 4^+ in Ref. [13] based on a polarization measurement from Compton scattering in Clover detectors. These asymmetry measurements are challenging with weaker, less clean lines. It is also not clear why no 1047 keV line was seen since it dominates the present coincidence spectrum shown in Fig. 1 as well as that of Fig. 1 in Ref. [12].

The first observation of the 3352 keV state may have been the weak peak at about 3345 keV tentatively assigned to ^{34}P in the $(t,^3\text{He})$ reaction [7]. It was reported again in Ref.

[12]. An assignment of $5\hbar \rightarrow 4\hbar$ provides an excellent fit to the angular distribution of the 1047 keV line with nearly zero mixing ratio. The only other spin hypothesis which provides a good fit is $3\hbar$. However, this relatively low spin is not consistent with the tendency of symmetric reactions like $^{18}\text{O} + ^{18}\text{O}$ to populate yrast and near yrast states. Its decay only to the 4^- state and its lifetime (see below) both imply negative parity. An assignment of 5^- , as suggested in Ref. [12] appears confident now. New states were observed at 3950, 4629, and 6192 keV which decay through newly reported transitions to the 2305 keV level. We have shown spin suggestions for these states based on systematics and shell model considerations discussed below, since we were unable to extract reliable angular distributions for the relevant transitions.

The angular distribution of the 2883 keV decay is consistent with either spin 6 or 7, but not 5, for the parent 6236 keV level. Spin 7 fits with a much smaller mixing ratio. Thus, our results are consistent with the earlier suggestion [12] of (7^+) .

B. Lifetimes

The mean lifetimes on a number of excited states were determined through a Doppler-shift analysis (DSA) of the lineshape data from LBNL which had better statistics at forward (40°) and backward (140°) angles. The code FITS [17] was used to simulate the production of ^{34}P in the thin ^{18}O layer and its slowing down and stopping in the thick Ta backing by numerical integration. The calculation used stopping powers obtained from the SRIM software package [18] (both nuclear and electronic interactions) for the incident ^{18}O beam slowing down in the thin ^{18}O target layer and for the recoil ^{34}P ions in both the remaining ^{18}O and in the Ta backing. The effects of energy and angular straggling, the finite size and resolution of the γ detectors, and the reaction kinematics were included in the simulation. Direct and side feeding were also taken into account.

Hypothetical mean lifetimes were varied to obtain the best agreement between simulated and measured lineshapes. The side-feeding times were also allowed to vary whenever the lifetimes of feeding transitions were known. Some examples of the lineshape fits are shown in Fig. 4.

The nucleus ^{34}P represents a particularly challenging case for DSA analysis because the lifetimes do not systematically decrease with increasing excitation energy due to the long

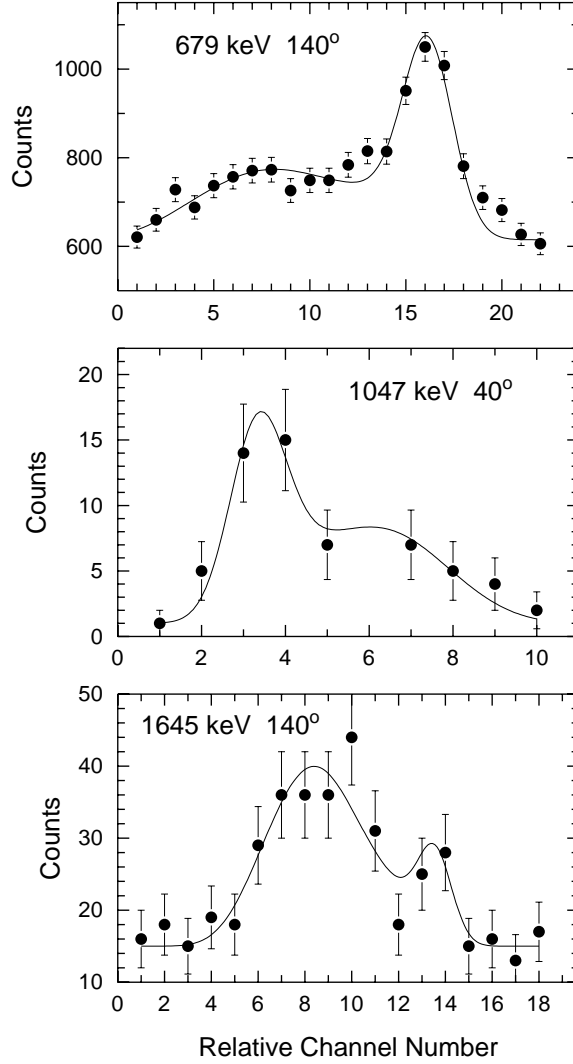


FIG. 4: Doppler-shift attenuation fits to the indicated γ lines observed at the indicated angles.

lifetimes of parity changing transitions from intruder configurations. The lineshapes for the 679, 1047, 1179, 1645, and 2325 keV transitions exhibited shifting within the range which can be fitted reliably by DSA analysis.. Some Doppler shifting was observed for the 429 and 2839 keV lines, but the long lifetime of the principal feeding transition to the 429 keV state (1876 keV) and limited statistics for the 2839 keV line only allowed the determination of upper limits to their lifetimes. No Doppler shifting was observed for the 1876, 1891, 2883 keV lines. This is consistent with the previously quoted limits of $0.3 < T_{1/2} < 2.5$ ns for the 2305 keV state (1876 keV transition) [12].

The lifetime values and limits are summarized in Table II along with the corresponding

TABLE II: Mean lifetimes measured in ^{34}P using the Doppler-shift attenuation method and corresponding electromagnetic transition strengths. The latter are based only on the lowest allowed multipolarity, *i.e.* zero mixing ratios. The lifetime range for the 2305 keV level was taken from Ref. [12]. The last column shows the electromagnetic transition strengths calculated in the shell model using the WBP-a interaction.

E_x (keV)	E_γ (keV)	J_i	J_f	Branch (%)	Mean τ (ps)	Multi- pole	B value (W.u.)	WBP-a (W.u.)
429	429	2 ⁺	1 ⁺	100	< 1.4	M1	> 0.3	0.3
1608	1179	1 ⁺	2 ⁺	64(9)	1.3(4)	M1	0.010(4)	0.005
	1607	1 ⁺	1 ⁺	36(9)		M1	0.002(1)	0.001
2305	1876	4 ⁻	2 ⁺	100	430 - 3600	M2	0.05 - 0.4	0.19
2320	1891	3 ⁻	2 ⁺	100	> 3	E1	< $5 \cdot 10^{-5}$	$4 \cdot 10^{-6}$
3352	1047	(5 ⁻)	4 ⁻	100	0.30(15)	M1	0.09(5)	0.02
3950	1645	(5 ⁻)	4 ⁻	100	0.30(15)	M1	0.02(1)	0.08
4629	679	(6 ⁻)	(5 ⁻)	40(11)	0.5(2)	M1	0.08(5)	0.18
	2325	(6 ⁻)	4 ⁻	60(11)		E2	2.2(1.4)	4
6192	2839	(6 ⁻)	(5 ⁻)	100	< 1	M1	> 0.001	0.1
6236	1607	(7 ⁺)	(6 ⁻)	75(8)	> 3	E1	< $6 \cdot 10^{-5}$	
	2883	(7 ⁺)	(5 ⁻)	25(8)		M2	< 2	

transition strengths. The latter are based on the assigned and suggested spins and parities. The branching ratios used are also shown in Table II. They are based on present measurements except for the 1608 keV level, whose branching ratios are taken from Ref. [8] because of the unresolved 1607 keV doublet. The transition strengths are for the lowest allowed multipolarities and assume zero mixing ratios. Small mixing ratios would not change these numbers significantly.

IV. DISCUSSION

With 19 neutrons, ^{34}P lies close to the shell closure at $N = 20$ and provides valuable data on the approach to the “island.” This can clearly be seen in Fig. 6 of Ref. [12] which compares the low-lying levels of $^{30,32,34,36}\text{P}$. The $3^-, 4^-$ doublet based primarily on the intruder $\pi s_{1/2} \otimes \nu f_{7/2}$ configuration falls steadily with increasing neutron number until reaching the ground state in ^{36}P , where it becomes the normal configuration in a simple shell model picture. The 4^- doublet member lies slightly lower except in ^{32}P . The remarkable almost perfect $N - Z$ dependence of the decrease in energy of the 4^- states among odd-odd nuclei approaching $N = 20$ is shown graphically in Fig. 18 of Ref. [5].

A consequence of the steady fall in the negative-parity intruder states across the P isotopes is a tendency not to see the positive-parity pure sd shell model states above them. This relates to the way many reactions (including the present one) populate yrast states preferentially and to the higher deformations and spins of the intruder states involving the relatively high spin $f_{7/2}$ orbital. The process appears to occur a second time for the (7^+) state at 6236 keV, which is likely a 2 particle-hole (2 ph) intruder state. It shows no Doppler shifting, which is highly unlikely for such a high energy M1 or E2 transition, but expected for an M2. A strong case is also made for the 7^+ assignment in the comparison of P isotopes in Fig. 6 of Ref. [12].

A. Shell Model

Shell model calculations [19] were first performed using the WBP interaction [20] which was optimized for lighter nuclei. The model space included unrestricted occupation of all orbitals in the sd shell and 0 or 1 particles above this shared between the $0f_{7/2}$ and $1p_{3/2}$ orbitals. The orbitals below particle number 8 were closed. Test calculations were also performed allowing one particle to move out of the $0p_{1/2}$ orbital or opening the $0f_{5/2}$ and $1p_{1/2}$ orbitals. There was only a small change in the calculated energies, occupancies, or transition strengths. The calculated occupancies of the orbitals are listed in Table III. Because of the model space limitations the positive-parity states cannot have any occupancy in the negative-parity p-f shell and thus are “normal” sd states. By construction of the interaction these states are identical to those predicted by the USD interaction. They are shown in the left

TABLE III: Subshell occupancies of states in ^{34}P calculated in the shell model with the WBP-a interaction, as discussed in the text.

E_x (keV)	J^π	NEUTRONS					PROTONS				
		0d _{5/2}	1s _{1/2}	0d _{3/2}	0f _{7/2}	1p _{3/2}	0d _{5/2}	1s _{1/2}	0d _{3/2}	0f _{7/2}	1p _{3/2}
0	1 ⁺	5.96	1.91	3.13			5.73	1.04	0.24		
363	2 ⁺	5.97	1.95	3.07			5.72	1.04	0.25		
1408	1 ⁺	5.95	1.40	3.65			5.56	1.06	0.38		
2216	2 ⁺	5.97	1.96	3.08			5.71	0.17	1.12		
2757	3 ⁺	5.93	1.95	3.13			5.69	0.26	1.05		
3788	4 ⁺	5.98	1.99	3.03			4.85	1.88	0.26		
2175	3 ⁻	5.81	1.68	2.52	0.90	0.09	5.43	0.98	0.58	0.01	0.00
2249	4 ⁻	5.80	1.71	2.49	0.96	0.04	5.45	1.07	0.48	0.00	0.00
2294	2 ⁻	5.80	1.72	2.48	0.30	0.69	5.52	0.90	0.57	0.00	0.00
2887	1 ⁻	5.80	1.73	2.48	0.13	0.86	5.45	1.12	0.42	0.00	0.00
3576	5 ⁻	5.81	1.62	2.57	0.98	0.02	5.32	0.59	1.08	0.00	0.00
3707	4 ⁻	5.82	1.66	2.53	0.45	0.55	5.31	1.25	0.43	0.00	0.00
3881	3 ⁻	5.79	1.58	2.63	0.65	0.33	5.29	0.99	0.71	0.00	0.00
4084	5 ⁻	5.80	1.66	2.54	0.95	0.05	5.22	1.27	0.50	0.00	0.00
4792	6 ⁻	5.80	1.71	2.49	0.95	0.04	5.31	1.25	0.44	0.01	0.00
4887	5 ⁻	5.79	1.60	2.62	0.89	0.11	5.33	0.81	0.85	0.01	0.00
5710	6 ⁻	5.79	1.59	2.63	0.98	0.01	5.13	0.77	1.10	0.00	0.00
6115	6 ⁻	5.86	1.83	2.32	0.95	0.04	5.15	1.30	0.54	0.01	0.00
7994	7 ⁺	5.78	1.69	1.81	1.12	0.60	5.24	0.94	0.54	0.27	0.01

column of the shell model levels in Fig. 2. Note that only states of spin 3⁺ or higher are shown above 5.5 MeV to reduce clutter. The intervening states can be seen in Fig. 5 of Ref. [12]. We see the first three predicted *sd* states in this experiment, although at slightly higher energies. The root-mean-square (RMS) difference between experiment and theory is 150 keV. The non-appearance at detectable levels of the higher *sd* states is almost certainly because they become non-yrast and heavy-ion reactions strongly favor yrast states.

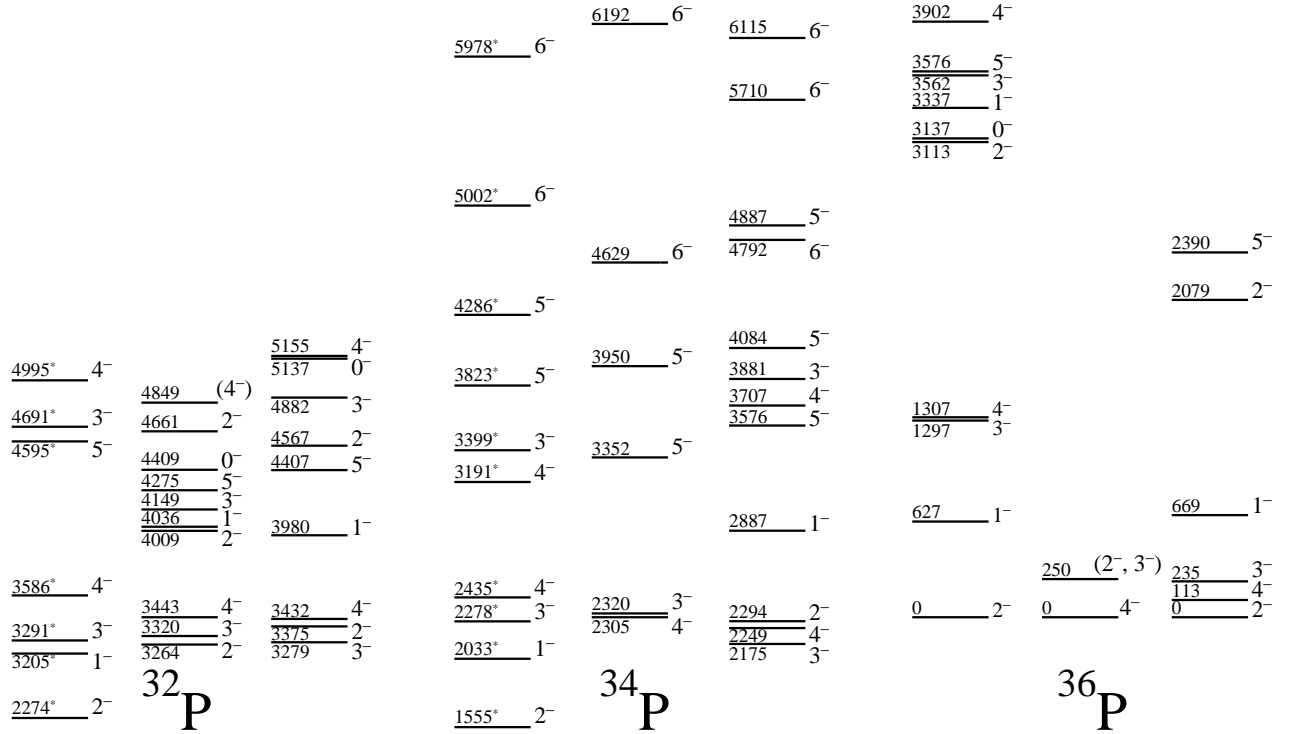


FIG. 5: A comparison of observed and calculated negative-parity states in some odd-odd P isotopes. In each group of 3, the WBP results are shown on the left, experiment in the middle, and WBP-a on the right. 1.5 MeV has been subtracted from all the WBP energies for $^{32,34}\text{P}$ (indicated by the *), whereas no adjustments have been made to the WBP-a results.

The orbital occupations in Table III confirm earlier speculation that the 1^+ ground state and lowest 2^+ state form a $\pi(s_{1/2}) \otimes \nu(d_{3/2})^{-1}$ doublet with nearly identical structure. Closer inspection does show some mixing into the $\pi d_{3/2}$ orbital from the lower $\pi d_{5/2}$ one. The 1_2^+ state shows a little more of this proton d shell mixing along with somewhat greater occupancy of the $\nu d_{3/2}$ orbital promoted from $\nu s_{1/2}$. There is significantly more $\pi d_{3/2}$ occupancy at the expense of the $\pi s_{1/2}$ orbital in the 2_2^+ and 3_1^+ predicted states (No experimental counterparts were observed for these states in the present experiment.) The lowest 4^+ state (proposed to account for the 2305 keV state in Ref. [13]) has a neutron structure almost identical to that of the ground state doublet, but with significantly increased occupancy of the $\pi s_{1/2}$ orbital at the expense of the lower $\pi d_{5/2}$ one.

The WBP calculations were not as satisfactory for the 1-ph negative-parity states. In Ref. [5] they were predicted about 1.2 MeV too high across the board. Calculations for

^{32}P , which is better known experimentally [21, 22] than ^{34}P , were about 1.5 MeV too high compared to the 0-ph states. Also the 2^- state was too low compared to the 3^- and 4^- ones. Examination of the shell occupancies revealed a high occupancy of the $1p_{3/2}$ orbital for the 2^- state (as would be expected for a $\pi 1s_{1/2} \otimes \nu 1p_{3/2}$ configuration) and significant $1p_{3/2}$ occupancy in the 3^- and 4^- levels which are expected to have a fairly pure $\pi 1s_{1/2} \otimes \nu 0f_{7/2}$ configuration. These considerations led us to examine the $0f_{7/2}$ and $1p_{3/2}$ single particle energies (SPE). These SPE were adjusted in the WBP interaction [20] to fit states in the $A = 20$ system, well below $A = 32$. We tried lowering the SPE for the $0f_{7/2}$ and $1p_{3/2}$ orbitals and found that reductions of 1.8 and 0.5 MeV, respectively, relative to the original WBP interaction in these SPE, provided a good fit to the energies of the negative-parity states in ^{32}P . There was no change at all in the energies or occupancies for the 0-ph states.

For purposes of discussion, we will call this modified interaction WBP-a. Energy levels predicted using both the WBP and WBP-a interactions are compared with experiment in Fig. 5 for the states with 1 particle above $N = 20$ in $^{32,34,36}\text{P}$. To make the comparison easier to see, 1.5 MeV has been subtracted from the WBP energies for $^{32,34}\text{P}$ in the spirit of Ref. [5]. (Note that for ^{36}P the ground state already has one neutron above $N = 20$, so the lowest state calculated is by definition the $E_x = 0$ ground state.) However, the WBP-a excitation energies are absolute relative to the lowest state with 0 (1) particles above $N = 20$ for $^{32,34}\text{P}$ (^{36}P) with nothing further subtracted. Clearly WBP-a brings the 1-ph states into good agreement with the experimental negative parity states in ^{32}P . In fact, the RMS difference between the experimental states and WBP-a calculations is 85 keV, a little lower than 150 keV for the positive-parity states. For ^{36}P the WBP-a calculation brings the lowest 4^- state down from 1307 keV (WBP) to 113 keV, which is within typical shell model deviations of 100 to 200 keV of the experimental result. Both the predicted 3^- and 2^- states are good candidates for the observed first excited state in ^{36}P . As a test, WBP-a calculations were also performed for 1-ph states in ^{30}Al . The lowest 4^- state was predicted at 2305 keV, very close in energy to the experimentally observed state at 2298 keV. This eliminated the need to subtract 1.2 MeV from the WBP energies, as was done in Ref. [5], and suggests that the WBP-a interaction may have a wider range of applicability.

The WBP and WBP-a results are also compared with the experimental levels in ^{34}P in Fig. 5. Because the WBP-a results agree better with the neighboring nuclei, we have shown these results for the 1-ph states in the right column of the shell model results in Fig. 2. The

predicted lowest 3^- and 4^- states agree reasonably well with the proposed experimental levels. The states are so close together in both theory and experiment that the reversed ordering is not significant. The two lowest predicted 5^- states agree reasonably well with the proposed experimental ones. The two experimental levels tentatively assigned 6^- also agree fairly well in energy with two of the lowest three WBP-a states. Overall, the RMS deviation between experiment and WBP-a results is about 145 keV, essentially the same as for the 0-ph states. These calculations based on an established interaction only slightly modified to fit a neighboring nucleus give more confidence in the spin-parity assignments. Most of the predicted states which have not been seen have lower spins and would have been populated significantly more weakly because the reaction favors yrast states. The same effect was seen in the $^{18}\text{O}(^{14}\text{C},\text{pn})^{30}\text{Al}$ reaction [5].

The lowest 3^- and 4^- states have nearly identical structures and conform moderately well with earlier speculations of a predominantly $\pi s_{1/2} \otimes \nu f_{7/2}$ composition. The neutron which is promoted into the $f_{7/2}$ shell comes predominantly from $d_{3/2}$, as would be expected, but with some contribution from both of the lower sd orbitals. The proton structure differs more from the simple expectation because about half a proton is promoted on average from the $d_{5/2}$ to the $d_{3/2}$ orbitals. By contrast the neutron occupancy of the lowest 2^- state is greatest in the $p_{3/2}$ orbital. The lowest 1^- state is even more purely a $\nu p_{3/2}$ state. No candidates were observed experimentally for the predicted 1^- or 2^- states, but similar states have been reported in ^{32}P . The proton occupancies of the three 5^- states differ mainly in the $s_{1/2}$ and $d_{3/2}$ orbitals while their neutron occupancies are almost identical to each other and to those of the lowest 3^- and 4^- states. Table III generally confirms the proposal in Ref. [12] of a stretched configuration of $\pi d_{3/2} \otimes \nu f_{7/2}$ for the lowest 5^- state, although the $0d_{3/2}$ proton which would usually be expected to come up from the $1s_{2/1}$ orbital also partly comes from the deeper $0d_{5/2}$ orbital. The occupancies of the three lowest 6^- states are rather similar to those of the lowest 5^- ones, including nearly 100% occupancy of a neutron in the $f_{7/2}$ orbital.

The predicted electromagnetic transition strengths are shown in the right column of Table II. Standard effective charges of 1.5 and 0.5 were used for protons and neutrons. There is good agreement with experiment. The B(M1) value for decay of the 429 keV state is relatively strong, while those from the 1608 keV 1^+ state are measured and predicted to be rather weak.

In reference to the assignment of 4^+ to the 2305 keV state [13], note that the nearest predicted 4^+ state lies nearly 1.5 MeV too high. This is well outside typical USD shell model predictions which are usually within 100 to 200 keV. Furthermore the M2 decay strength which a 4^- assignment would imply is well within the possible lifetime range reported in Ref. [12]. In contrast, the 4^+ assignment would imply a B(E2) strength in the range of 0.002 to 0.01 W.u. which is about 3 orders of magnitude below the shell model value of 4.5 W.u. (This value of 4.5 W.u. equates to $29 e^2 fm^4$, about two orders of magnitude greater than the value of $0.247 e^2 fm^4$ reported in Ref. [13]. We don't understand this difference. The effective charges used in Ref. [13] of 1.3 for protons and 0.5 or 0.3 for neutrons lead to only moderate reductions of the B(E2) values to 3.4 or 3.2 W.u., respectively, in the present shell model calculations.)

The lowest 0-ph 7^+ state is predicted to lie at 11.4 MeV, over 5 MeV above the experimental 6236 keV level. The lowest 7^+ state predicted by the WBP-a interaction with 2 neutrons above $N = 20$, lies at 8230 keV or 2 MeV higher than experiment. However, this is not the lowest 2-ph state. A 6^+ state is predicted 580 keV lower. Mixing with the 0-ph states would lower these energies somewhat but would not necessarily favor the 7^+ level. An assignment of 6^+ is not consistent with the measured angular distribution of the 6236 keV state. Even if all the 2-ph states were lowered in energy enough to bring the predicted 7^+ one into agreement with experiment, some predicted 6^+ states would lie lower and provide a very fast decay path for the 7^+ state. This would be inconsistent with its observed decay modes and long lifetime. A clue to a more likely explanation is the predicted 0.27 $\pi f_{7/2}$ occupancy of the WBP-a 7^+ state. This is unusual because the neutron Fermi level lies much higher than that for protons and there is essentially no proton occupancy above $N = 20$ in any of the other 1-ph or 2-ph states calculated. Although the $\pi f_{7/2}$ occupancy is still well below unity, it begins to suggest the fully aligned $\pi f_{7/2} \otimes \nu f_{7/2}$ configuration previously proposed. Perhaps the WBP-a interaction just doesn't favor such a fully aligned state as much as is seen in experiment. This may be an issue with the 2-body matrix elements whose adjustment is beyond the scope of the present work.

V. SUMMARY

Excited states in ^{34}P were studied following its population in the $^{18}\text{O}(^{18}\text{O},\text{pn})$ reaction at laboratory energies of 20, 24, 25, 30, and 44 MeV at Florida State University and at Lawrence Berkeley National Laboratory. Most previously reported states were confirmed and new ones were observed. Angular distributions were measured for a number of the decay transitions, and mean lifetimes were determined by analyzing the Doppler-shifted lineshapes. A number of new transitions, levels, and spin assignments were determined.

The results were compared to shell model calculations using the WBP-a interaction. This is the traditional WBP interaction which was crafted for nuclei in the $A = 10$ to 20 range, but with a reduction of the $f_{7/2}$ and $p_{3/2}$ SPE by 1.8 and 0.5 MeV, respectively, to better fit the $A = 32$ to 36 region. The first 3 states agree fairly well with the predictions for 0-ph configurations, which are identical to those for pure sd states using the USD interaction. The next 6 states are reproduced equally well by the 1-ph calculations (1 nucleon in the fp shell). The highest state near the neutron separation energy is an excellent candidate for a 2-ph 7^+ state. The lowest 7^+ state in the 2-ph WBP-a calculations is still 2 MeV too high, but its wavefunction hints at a fully aligned $\pi f_{7/2} \otimes \nu f_{7/2}$ configuration which may be more energetically favored than in the calculation.

Acknowledgments

This work was supported in part by the National Science Foundation through grant numbers PHY-04-56463 and PHY-07-56474. Support for Lawrence Berkeley National Laboratory was provided by the U.S. Department of Energy under Contract No. DE-AC02-05CH11231. Part of this work was performed under the auspices of the U.S. Department of Energy by the University of California, Lawrence Livermore National Laboratory under Contract W-7405-Eng-48 and under Contract DE-AC52-07NA27344.

-
- [1] C. Thibault, R. Klapisch, C. Rigaud, A. M. Poskanzer, R. Prieels, L. Lessard, and W. Reisdorf, *Phys. Rev. C* **12**, 644 (1975).
 - [2] E.K. Warburton, J.A. Becker, and B. A. Brown, *Phys. Rev. C* **41**, 1147 (1990).

- [3] T. Otsuka, R. Fujimoto, Y. Utsuno, B.A. Brown, M. Honma, and T. Mizusaki, *Phys. Rev. Lett.* **87**, 082502 (2001).
- [4] T. Otsuka, T. Suzuki, R. Fujimoto, H. Grawe, and Y. Akaishi, *Phys. Rev. Lett.* **95**, 232502 (2005).
- [5] T. A. Hinnners, V. Tripathi, S.L. Tabor, A. Volya, P.C. Bender, C.R. Hoffman, S. Lee, M. Perry, P.F. Mantica, A.D. Davies, S.N. Liddick, W.F. Mueller, A. Stolz, and B.E. Tomlin, *Phys. Rev. C* **77**, 034305 (2008).
- [6] D. R. Goosman, C. N. Davids, and D. E. Alburger, *Phys. Rev C* **8**, 1324 (1973).
- [7] F. Ajzenberg-Selove, E. R. Flynn, and J. W. Sunier, *Phys. Rev C* **15**, 1 (1977).
- [8] A. M. Nathan and D. E. Alburger, *Phys. Rev. C* **15**, 1448 (1977).
- [9] P.V. Drumm, L.K. Fifield, R.A. Bark, M.A.C. Hotchkis, C.L. Woods, and P. Maier-Komor, *Nucl. Phys.*, **A441**, 95, 1985.
- [10] B. Fornal, R.H. Mayer, I.G. Bearden, Ph. Benet, R. Broda, P.J. Daly, Z.W. Grabowski, I Ahmad, M.P. Carpenter, P.B. Fernandez, R.V.F. Janssens, T.L. Khoo, T. Lauritsen, E.F. Moore, and M. Drigert, *Phys. Rev. C* **49**, 2413 (1994).
- [11] B.V. Pritychenko, T. Glasmacher, B.A. Brown, P.D. Cottle, R.W. Ibbotson, K.W. Kemper, and H. Scheit, *Phys. Rev. C* **62**, 051601(R) (2000).
- [12] J. Ollier, R. Chapman, X. Liang, M. Labiche, K.-M. Spohr, M. Davison, G. de Angelis, M. Axiotis, T. Kröll, D. R. Napoli, T. Martinez, D. Bazzacco, E. Farnea, S. Lunardi, A. G. Smith, and F. Haas, *Phys. Rev. C* **71**, 034316 (2005).
- [13] Krishichayan, A. Chakraborty, S. Mukhopadhyay, S. Ray, N. S. Pattabiraman, S. S. Ghugre, R. Goswami, A. K. Sinha, S. Sarkar, U. Garg, P.D. Madhusudhana, S.K. Basu, B.K. Yogi, L. Chaturvedi, A. Dhal, R.K. Sinha, M. Saha Sarkar, S. Saha, R. Singh, R.K. Bhomik, A. Jhingan, N. Madhavan, S. Muralithar, S. Nath, R.P. Singh, and P. Sugathan, *Eur. Phys. Jour. A* **29**, 151 (2006).
- [14] G. Duchêne, F. A. Beck and P. J. Twin, G. de France, D. Curien, L. Han, C. W. Beausang, M. A. Bentley, P. J. Nolan, and J. Simpson, *Nuclear Instruments and Methods in Physics Research Section A: Accelerators, Spectrometers, Detectors and Associated Equipment* **432**, 98 (1999).
- [15] Z. Elekes, T. Belgya, G. L. Molnár, Á. Z. Kiss, M. Csatlós, J. Gulyás, A. Krasznahorkay, and Z. Máté, *Nuclear Instruments and Methods in Physics Research Section A: Accelerators,*

Spectrometers, Detectors and Associated Equipment **503**, 580 (2003).

- [16] M. Wiedeking, P. Fallon, A. O. Macchiavelli, L. A. Bernstein, J. Gibelin, L. Phair, J. T. Burke, D. L. Bleuel, R. M. Clark, M. A. Deleplanque, S. Gros, R. Hatarik, H. B. Jeppesen, I.-Y. Lee, B. F. Lyles, M. A. McMahan, L. G. Moretto, J. Pavan, E. Rodriguez-Vieitez, and A. Volya, *Phys. Rev. C* **77**, 054305 (2008).
- [17] E.F. Moore, P.D. Cottle, C.J. Gross, D.M. Headly, U.J. Hüttmeier, S.L. Tabor, and W. Nazarewicz, *Phys. Rev. C* **38**, 696 (1988).
- [18] Web site: <http://www.SRIM.org> (2008); J. F. Ziegler, J.P. Biersack, and U. Littmark, “The stopping and range of ions in matter” (Pergamon, New York, 1985).
- [19] D. Morris and A. Volya, web site: <http://cosmo.volya.net> (2008).
- [20] E.K. Warburton and B.A. Brown, *Phys. Rev. C* **46**, 923 (1992).
- [21] Web site: <http://www.nndc.bnl.gov/ensdf> (2009).
- [22] P. Baumann, A.M. Bergdolt, G. Bergdolt, R. M. Freeman, F. Haas, B. Heusch, A. Huck, and G. Walter, *Fizika (Suppl.)* **10**, 11 1978.

DISCLAIMER

This document was prepared as an account of work sponsored by the United States Government. While this document is believed to contain correct information, neither the United States Government nor any agency thereof, nor The Regents of the University of California, nor any of their employees, makes any warranty, express or implied, or assumes any legal responsibility for the accuracy, completeness, or usefulness of any information, apparatus, product, or process disclosed, or represents that its use would not infringe privately owned rights. Reference herein to any specific commercial product, process, or service by its trade name, trademark, manufacturer, or otherwise, does not necessarily constitute or imply its endorsement, recommendation, or favoring by the United States Government or any agency thereof, or The Regents of the University of California. The views and opinions of authors expressed herein do not necessarily state or reflect those of the United States Government or any agency thereof or The Regents of the University of California.